

Assessment of Therapeutic Tumor Response Using ^{99m}Tc -Ethylenedicysteine-Glucosamine

David Yang, Masashi Yukihiro, Dong-Fang Yu, Megumi Ito, Chang-Sok Oh, Saady Kohanim, Ali Azhdarinia, Chang-Guhn Kim, Jerry Bryant, E. Edmund Kim, and Donald Podoloff

Division of Diagnostic Imaging, The University of Texas M.D. Anderson Cancer Center, Houston, TX

ABSTRACT

Purpose: The aim of this study was to evaluate ^{99m}Tc -ethylenedicysteine-glucosamine (EC-DG) for the assessment of tumor growth. **Method:** To evaluate whether ^{99m}Tc -EC-DG is involved in cell nuclei activity, in vitro thymidine incorporation, and cell-cycle assays of EC-DG were conducted using lung and breast cancer cells. Biodistribution of ^{99m}Tc -EC-DG in lung tumor-bearing mice (0.5–4 hours, 1 $\mu\text{Ci}/\text{mouse}$, i.v.) was used to estimate the radiation-absorbed dose. Autoradiograms of ^{99m}Tc -EC-DG and ^{18}F -FDG were compared in nude mice bearing uterine sarcoma. Rabbits inoculated with VX-2 cells were imaged with ^{99m}Tc -EC-DG and ^{99m}Tc -EC. For therapeutic assessment studies, scintigraphic imaging studies with ^{99m}Tc -EC-DG in mammary tumor-bearing rats were conducted at various days after treatment with paclitaxel and cisplatin. The imaging findings were correlated immunohistochemical assays (mRNA expression, apoptosis, and cell-cycle changes in tumor), and flow cytometry analysis was performed. **Results:** In vitro cellular uptake assays indicated that cell nuclei activity could be assessed by ^{99m}Tc -EC-DG. Scintigraphy and autoradiograms in animal models demonstrated that the tumor could be clearly visualized by ^{99m}Tc -EC-DG. The efficacy of paclitaxel and cisplatin treatment in rodent models could be assessed using tumor/muscle ratios. Immunohistochemical staining indicated a reduced expression of bFGF and an increased apoptosis and cell-cycle changes after paclitaxel and cisplatin treatment. **Conclusion:** ^{99m}Tc -EC-DG is involved in cell nuclei activity and could assess the therapeutic tumor response.

Key words: ^{99m}Tc -EC-DG, biodistribution, imaging

INTRODUCTION

Radionuclide imaging modalities (positron emission tomography [PET] and single photon emission computed tomography [SPECT]) are used to map the location and concentration of radionuclide-labeled compounds.^{1–3} Among all radioiso-

topes, ^{99m}Tc has been preferred to label radiopharmaceuticals because of favorable low energy (140 Kev versus 511 Kev for ^{18}F) and inexpensive isotope cost (\$0.21/mCi versus \$30–\$50/mCi for ^{18}F). Several ^{99m}Tc -labeling techniques have been reported, such as N_4 (e.g., DOTA), N_3S (e.g., MAG-3), N_2S_2 (e.g., ECD), NS_3 , S_4 (e.g., sulfur colloid), diethylenetriamine penta-acetic acid (DTPA), and hydrazineticotinamide (HYNIC).^{4–10} Among these chelators, the HYNIC technique requires two additional chemicals (tricine, triphenylphosphine) in order to form a ^{99m}Tc complex, thus making it inconvenient and costly. The nitrogen and sulfur combination has been shown to be a stable chelator for

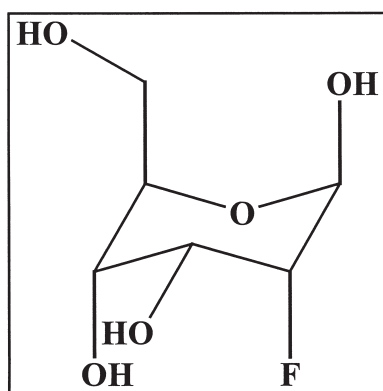
Address reprint requests to: David Yang; Department of Nuclear Medicine, Box 59, The University of Texas M.D. Anderson Cancer Center; 1515 Holcombe Boulevard, Houston, TX 77030; Tel.: 713-794-1053; Fax: 713-794-5456

E-mail: dyang@di.mdacc.tmc.edu

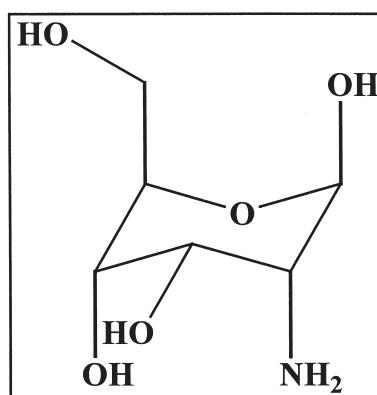
^{99m}Tc . Bis-aminoethanethiol tetradentate ligands, also called diaminodithiol compounds, are known to form very stable Tc(V)O -complexes on the basis of efficient binding of the oxotechnetium group to two thiol-sulfur and two amine nitrogen atoms. ^{99m}Tc -L,L-ethylenedicysteine (^{99m}Tc -EC) is the most recent and successful example of N_2S_2 chelates. EC can be labeled with ^{99m}Tc easily and efficiently with high radiochemical purity and stability.^{11,12} We have previously reported a series of ^{99m}Tc -EC-agent conjugates for functional imaging in oncology.^{13–20} In addition, EC can also be labeled with ^{68}Ga for PET imaging and ^{188}Re (a beta and gamma emitter) for internal radionuclide therapy.^{21–23} ^{99m}Tc , ^{68}Ga , and ^{188}Re are generator-produced isotopes that are accessible and affordable.

There is a structural similarity between FDG and glucosamine (structure shown in Fig. 1). At

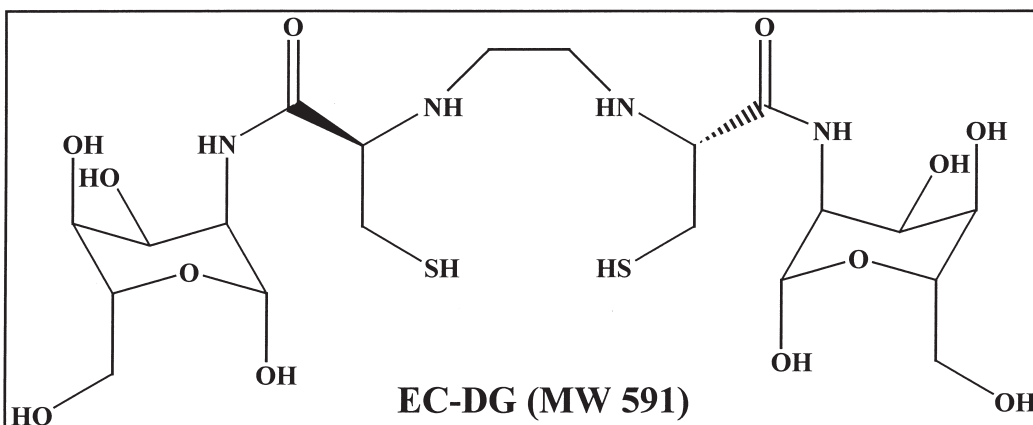
position 2 of the sugar, FDG and glucosamine have the fluorine and amino group, respectively. Similar to FDG, the cellular uptake of glucosamine is by a glucose transporter process.¹⁹ However, its regulatory products of glucosamine-6-phosphate mediate insulin activation, downstream signaling, and translocation, which upregulate mRNA expression and tumor growth.^{24,25} For instance, Sp-1 is one of the known transcription factors whose activity may be post-translationally triggered by glucosamine.^{26–28} Sp-1 binding sites are possible to be present in the promoters of potent angiogenic growth factors, such as VEGF and IL-8, and regulate oncogenic factors with cell-cycle factors at the basal level of transcription or repression. Therefore, radiolabeled glucosamine may be able to noninvasively assess cell nuclei activity and characterize tumor growth. We have then developed ^{99m}Tc -EC-glucosamine



FDG (MW 182)



D-Glucosamine (MW 179)



EC-DG (MW 591)

Figure 1. Chemical structures and molecular weights of fluorodeoxyglucose (FDG), D-glucosamine, and ethylenedicysteine-deoxyglucose (EC-DG).

(^{99m}Tc -EC-DG) for tumor tissue-specific targeted imaging.

Results from our animal studies showed that the binding of ^{99m}Tc -EC-DG in tumors can be imaged.¹⁹ Our ^{99m}Tc -EC-DG instant kit has obtained IRB (ID 01-415) and IND (#63,698) approval from the University of Texas M.D. Anderson Cancer Center and the Food and Drug Administration (FDA). A phase I trial, using ^{99m}Tc -EC-DG to image tumors in patients with head, neck, and lung cancer, is in progress. In this paper, we evaluated the role of ^{99m}Tc -EC-DG in chemotherapeutic response assessment in animal models. Paclitaxel (Sigma Chemical Co., St. Louis, MO) and cisplatin were selected in the animal studies because they have demonstrated significant antitumor effect against mammary tumors.^{29–36} Paclitaxel increases microtubule stability by preventing tubulin depolymerization, which results in tubulin bundling.^{31,32} Paclitaxel also mediates a direct antiangiogenic effect against several cell lines.^{33,34} Cisplatin has been involved in cell-cycle arrest in various types of tumor cells.^{35,36} The correlation of biologic markers with the tumor uptake of ^{99m}Tc -EC-DG was studied.

MATERIALS AND METHODS

Synthesis of Ethylenedicysteine (EC)

Cysteine-HCl (41.52 g) was dissolved in water (106 mL). To this solution, formaldehyde was added (26.1 mL), and the reaction mixture was stirred overnight at room temperature. Pyridine (26.6 mL) was then added and the precipitate formed. The crystals were separated and washed with ethanol (54 mL) for 25 minutes at room temperature, then filtered with a Buchner funnel. The crystals were triturated with petroleum ether (150 mL), again filtered, and then lyophilized for 3 days. The precursor, L-thiazolidine-4-carboxylic acid (m.p. 195°C, reported 196°C–197°C), was used for the synthesis of EC. The precursor (22 g) was dissolved in liquid ammonia (200 mL) and refluxed. Sodium metal was added until a persistent blue color appeared. Ammonium chloride was added to the blue solution, and then the solvents were evaporated to dryness. The residue was dissolved in water (200 mL), and the pH was adjusted to 2. A precipitate formed and was filtered and washed with water (500 mL). The solid was dried in a calcium chloride dessicator. EC was then prepared (m.p. 243°C–246°C, reported 251°C–253°C).

Synthesis of ^{99m}Tc -ethylenedicysteine-Glucosamine (^{99m}Tc -EC-DG)

EC was conjugated to glucosamine according to an established method, as described in our previous literature.¹⁹ Briefly, sodium hydroxide (1N, 1 mL) was added to a stirred solution of EC (110 mg, 0.41 mmol) in water (5 mL). To this colorless solution, sulfo-N-hydroxysuccinimide (Pierce Chemical Co., Radford, IL) (241.6 mg, 1.12 mmol) and 1-ethyl-3-(3-dimethylamino-propyl)carbodi-imide-HCl (Aldrich Chemical Co., Milwaukee, WI) (218.8 mg, 1.15 mmol) were added. D-Glucosamine hydrochloride salt (Sigma Chemical Co., St. Louis, MO) (356.8 mg, 1.65 mmol) was then added. The mixture was then stirred at room temperature for 24 hours. The mixture was then filtered through a 0.45 micron filter, and the pH of the solution was adjusted to 6.4–7.0. To remove the unreacted starting materials, the mixture was dialyzed for 48 hours using Spectra/POR molecular porous membrane, with the cut-off at 500 (Spectrum Medical Industries Inc., Houston, TX). After dialysis, the product was freeze-dried using a lyophilizer (Labconco, Kansas City, MO). The product weighed 291 mg (yield 60%). Proton-NMR (D_2O) δ 2.60–2.90 (m, 4H and -CH₂-SH of EC), 2.95 (t, 2H, glucosamine 5-CH-CH₂OH) 3.20 (d, 4H, glucosamine 6-CH₂OH), 3.30–3.95 (m, 6H glucosamine 1,3,4-CH and 4H CH₂-SH of EC) 3.30–3.66 (m, 4H, CH₂-CH₂- of EC), 4.15–4.30 (t, 2H, NH-CH-CO of EC), 4.60 (d, 2H, glucosamine 2-CH-NH₂). FAB MS *m/z* 591 (M^+ , 20).

The radiosynthesis of ^{99m}Tc -EC-DG was achieved by adding ^{99m}Tc -pertechnetate (40–50 mCi) into the lyophilized residue of EC-DG (50 mg) and tin (II) chloride (SnCl_2 , 100 μg). The complexation of EC-DG with ^{99m}Tc was carried out at a pH of 6.5. Radiochemical purity was determined by TLC (ITLC SG, Gelman Sciences, Ann Arbor, MI) eluted with ammonium acetate (1M in water):methanol (4:1). High-performance liquid chromatography (HPLC), equipped with a NaI detector and UV detector (254 nm), was performed on a gel permeation column (Biosep SEC-S3000, 7.8 \times 300 mm, Phenomenex, Torrance, CA) using a flow rate of 1.0 mL/min. The eluant was 0.1% LiBr in phosphate buffered saline (PBS) (10 mM, pH = 7.4). The stability of the ^{99m}Tc -EC-DG kit was tested in serum samples. Briefly, ^{99m}Tc -EC-DG (100 μCi) was incubated in dog serum (200 μl) at 37°C at 0.5–24

hours. The serum samples were diluted with 50% methanol in water, and radio-TLC was used to analyze the product.

***In Vitro* [³H]Thymidine Incorporation and Cell-Cycle Assays**

Previous studies have shown that the cellular uptake of ^{99m}Tc-EC-DG was by a glucose-mediated process.¹⁹ ^{99m}Tc-EC-DG may share the same pathway as glucose. To demonstrate if EC-DG and glucose are involved in cancer cells' proliferation or growth, thymidine incorporation assays were conducted. ^{99m}Tc-EC-DG is a tumor-seeking agent that can image various tumor types. Thus, we used different cancer cells in various studies. Thymidine incorporation assays were conducted in lung cancer cells. Briefly, human lung tumor cells (A549) were plated at 50,000 cells/well in 1 mL RPMI-1640. Unlabeled EC-DG raw material, FDG, and d-glucose (0.1–1 mg in 20 μ l/well) (Aldrich Chemical Co., Milwaukee, WI) and saline (control) were added to this 12-well culture plate and incubated in 5% CO₂/air at 37°C. After 24 hours, each well was washed with sterile PBS, and fresh RPMI-1640 was added to each well. Each well was applied with 0.5 μ Ci/10 μ l saline of [³H]thymidine and incubated for 24 hours. Finally, each well was washed with ice-cold PBS and trypsinized with 100 μ L of trypsin and incubated for 10 minutes in the incubator. The mixture was filtered through a cell harvester. The filters containing cells were added with the cocktail, and radioactivity was counted. The cellular uptake of [³H]thymidine in the control group was unified to be 100 (baseline).

To determine whether EC-DG is involved in the cell-cycle process, breast cancer cells were used in this study. Briefly, breast cancer cells (20 M, adherent) were cultured in RPMI-1640 in a T75 flask. The cells were washed with PBS twice, and serum-free media was added. Hoechst 33342 (5 μ L) per 1 mL of RPMI-1640 (stock solution: 1 mg/ml) was added. The media was aspirated and washed with PBS. The cells were trypsinized, collected, and sorted. The sorted cells were plated to a 12-well plate (50,000 cells/well), and 4 μ Ci of ^{99m}Tc-EC-DG, ^{99m}Tc-EC, or ¹⁸F-FDG (CTI Co., Houston, TX) were added. The specific activity of ^{99m}Tc-EC-DG and ^{99m}Tc-EC was 25 mg/5 mL/mCi. After incubation for 2 hours, cells were washed with ice-cold PBS and trypsinized. Then, cells were collected and the radioactivity was measured by a gamma counter.

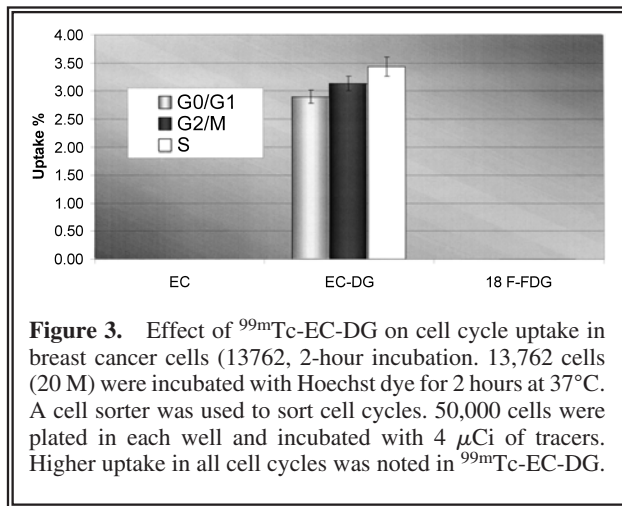
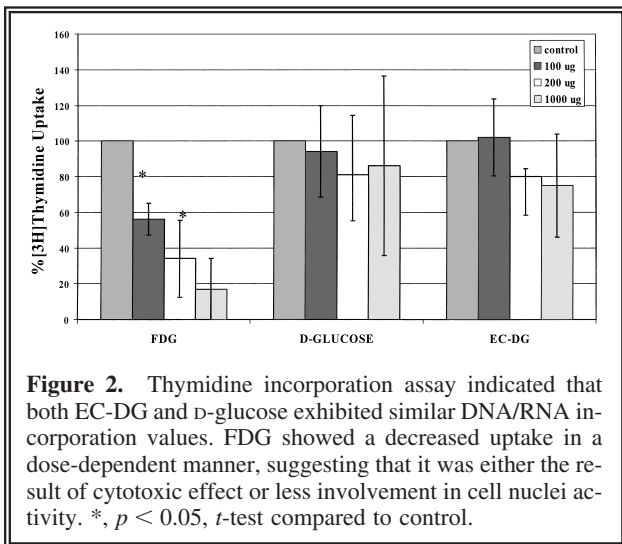
Effect of Transchelators on the Cellular Uptake of the ^{99m}Tc-EC-DG Kit

To determine the effect of transchelators on the cellular uptake of the ^{99m}Tc-EC-DG kit, ^{99m}Tc-pertechnetate was added into a homemade kit containing the lyophilized residue of EC-DG (5 mg) and tin (II) chloride (SnCl₂, 100 μ g in 0.1 mL water) and gluconate or glucarate (Aldrich Chemical Co., Milwaukee, WI) (10%–40% w/w of EC-DG). The complexation of EC-DG with ^{99m}Tc was carried out at a pH of 6.5. Radiochemical purity was determined by ITLC eluted with ammonium acetate (1 M in water):methanol (4:1). Breast cancer cell line (13762) was used in these assays. The cell line was obtained from American Type Culture Collection (Rockville, MD). The cells were plated to a 12-well tissue-culture plate that contained 50,000 cells/well. The cells were incubated with sodium gluconate or sodium glucarate (10–40 μ g/well, with a concentration of 0.5–2mg/mL, 10%–40% w/w per well) for 30 minutes, followed by adding 4 μ Ci (0.148 MBq) of ^{99m}Tc-EC-DG (0.1 mg/well, with a concentration of 5 mg/mL) to each well, and the cells were incubated at 37°C for 2 hours. Control groups were ^{99m}Tc-gluconate and ^{99m}Tc-glucarate (0.1 mg/well, with a concentration of 5 mg/mL). After incubation, the cells were washed with ice-cold PBS twice and trypsinized with 0.5 mL of trypsin solution. Then, the cells were collected, and the radioactivity was measured by a gamma counter (Packard Instruments, Downers Grove, IL). Data were expressed in mean \pm standard deviation (SD) percent of uptake (4 μ Ci = 100%) of three measurements.

Dosimetry of ^{99m}Tc-EC-DG Kit in Tumor-Bearing Mice

The animals were housed in The University of Texas M.D. Anderson Cancer Center facility. All protocols involving animals were approved by the M.D. Anderson Animal Use and Care Committee. Athymic nude mice (20–25 g) were inoculated subcutaneously with 0.1 mL of human lung tumor cells (A549, 10⁶ cells/mouse) into the hind legs, using 25-gauge needles. Biodistribution studies were performed 17–21 days after implantation, when tumors reached approximately 0.6 cm in diameter.

Each animal was injected intravenously (i.v.) with 1–2 μ Ci (per mouse) of ^{99m}Tc-EC-DG containing 20% gluconate (n = 3 mice/time point). Gluconate concentration was obtained from the



in vitro studies, as described in the above text. The physical amounts of EC-DG, gluconate, and SnCl_2 used were 5 mg, 1 mg, and 0.1 mg, respectively. The radioactivity concentration and i.v. injection volume were 0.2 mCi/10 mL and 0.1 mL/mouse. At 0.5–4 hours following the administration of ^{99m}Tc -EC-DG, the rodents were sacrificed.

Radioactivity in each sample tissue was calculated as the percentage of the injected dose per gram of tissue wet weight (%ID/g).¹⁹ Dosimetric calculations were performed using time-activity curves, which were generated for each organ. Analytic integration of the curves was used to determine the area under the curve (AUC), which was then divided by injected dose to yield the residence time of each organ. Residence times were then used to calculate the target organ-absorbed radiation doses based on the MIRD methodology for the normal adult male, using the MIRDose 3.1 software package (Oak Ridge Institute for Science and Education, Knoxville, Tennessee).³⁷

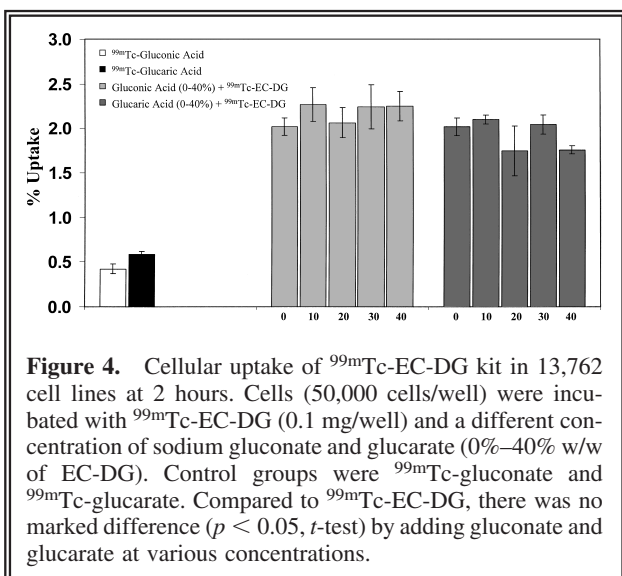
Autoradiographic Studies

^{99m}Tc -EC-DG containing 20% gluconate was used in this study. The physical amounts of EC-DG, gluconate, and SnCl_2 used in autoradiographic studies were 5 mg, 1 mg, and 0.1 mg, respectively. The radioactivity concentration and i.v. injection volume were 1 mCi/mL and 0.1 mL/mouse. Following an i.v. injection of 100 μCi of ^{99m}Tc -EC-DG and ^{18}F -FDG, uterine tumor-bearing nude mice were killed at 1 hour, and the body was fixed in carboxymethyl cellulose (3%). The frozen body was mounted onto a cryo-

stat (LKB 2250 cryomicrotome) and cut into 100- μm coronal sections. Each section was thawed and mounted on a slide. The slide was then placed in contact with a multipurpose phosphor storage screen (Cyclone Storage Phosphor System, Packard, Meridian, CT) and exposed for 15 hours.

Gamma Scintigraphic Imaging Studies in VX-2 Tumor-Bearing Rabbits

New Zealand White Rabbits (2.5–3 kg) were inoculated with VX-2 tumor mass (rabbit-driven squamous mammary tumor) using 18-gauge needles. The rabbits were administered i.v. ^{99m}Tc -EC-DG (containing 20% gluconate) or ^{99m}Tc -EC (control). The physical amounts of



EC-DG, gluconate, and SnCl₂ used in imaging studies were 5 mg, 1 mg, and 0.1 mg, respectively. The radioactivity concentration and injection volume were 1 mCi/mL and 1 mL/rabbit. Rabbits were anesthetized using isoflurane and positioned supine, and scintigraphic images were obtained using a 2020tc Imager gamma camera from Digirad (San Diego, CA). The camera was equipped with a low-energy, parallel-hole collimator. The field of view of Digirad is 20 cm × 20 cm, with an edge of 1.3 cm. The intrinsic spatial resolution is 3 mm, and the matrix is 64 × 64. With a low-energy, high-resolution collimator installed (as required with ^{99m}Tc), the system is designed for a planar sensitivity of at least 125 counts/minute (cpm)/μCi and a spatial resolution of 7.6 mm.

Therapeutic Response Assessment

On day 14 postinoculation, mammary tumor-bearing rats (150–175 g, n = 5 rats/agent) were administered a single i.v. injection of Taxol (20 mg/kg) or saline. On day 23 postinoculation (9 days post-therapy), tumor-bearing rats were imaged with a ^{99m}Tc-EC-DG kit (300 μCi/rat, i.v.) at 0.5–2 hours after administration. The physical amounts of EC-DG, gluconate, and SnCl₂ used in imaging studies were 5 mg, 1 mg, and 0.1 mg, respectively. The radioactivity concentration and injection volume were 1 mCi/mL and 0.3 mL/rat. After the imaging procedures were completed, the rats were killed and tumor lesions were removed for immunohistochemical staining,¹⁷ in order to assess the antiangiogenic effect of the therapy. A similar study was conducted using cisplatin (CDDP). Mammary tumor-bearing rats were treated with CDDP (4 and 8 mg/kg, i.p.) on day 14. In these rats, gamma images were acquired on days 14 (baseline), 18, and 39 postinoculation. Computer-outlined regions of interest (ROI) (counts per pixel) of the tumor lesion site and the symmetric normal muscle site were used to determine tumor-to-background count/density ratios. The ratios were used to compare dynamic tumor uptake pre- and post-treatment. To assess locoregional radioactivity, a small handheld gamma camera (eZ-SCOPE, Anzai Medical Co., Ltd., Tokyo, Japan) was also used with a low-energy, parallel-hole collimator (high-sensitive type). The field of view for eZ-SCOPE is 32 mm × 32 mm with 16 × 16 pixels, of which intrinsic spatial resolution is 2 mm and sensitivity is 770,000 cps/MBq.

The effects of Taxol and CDDP on cell-cycle

distribution and percentage of apoptotic cells was determined by flow cytometric and immunofluorescence assays (fluorescence activated cell sorter; FACS), using known procedures.³⁸ At 72 hours after incubation with Taxol or CDDP (1 μg), mammary tumor cells (10⁶ cells/well) were stained with 2.5% propidium iodide solution/0.3% saponin/0.001% RNase A in 10 mM EDTA. Stained nuclei were analyzed by using a Coulter EPICS XL-MCL (Coulter Corp., Miami, FL) for the proportions of cells in the G₀/G₁, S, and G₂-M phases of the cell cycle. Cell-cycle studies were conducted three times. The presence of

Table 1. Estimated Dosimetry of ^{99m}Tc-EC-Deoxyglucose

<i>Target organ</i>	<i>mGy/MBq</i>	<i>rad/mCi</i>
Adrenals	5.06E-03	1.87E-02
Brain	7.92E-06	2.93E-05
Breasts	5.62E-04	2.08E-03
Gallbladder wall	7.06E-03	2.61E-02
LLI Wall	2.60E-04	9.63E-04
Small intestine	1.39E-03	5.13E-03
Stomach	2.01E-03	7.44E-03
ULI wall	1.88E-03	6.96E-03
Heart wall	2.06E-03	7.61E-03
Kidneys	3.76E-02	1.39E-01
Liver	2.30E-02	8.50E-02
Lungs	2.00E-03	7.41E-03
Muscle	8.20E-04	3.03E-03
Ovaries	4.58E-04	1.69E-03
Pancreas	4.49E-03	1.66E-02
Red marrow	1.06E-03	3.91E-03
Bone surfaces	1.33E-03	4.94E-03
Skin	3.64E-04	1.35E-03
Spleen	1.24E-02	4.57E-02
Testes	1.97E-05	7.29E-05
Thymus	5.15E-04	1.90E-03
Thyroid	1.21E-03	4.49E-03
Urin bladder wall	1.31E-04	4.86E-04
Uterus	4.01E-04	1.48E-03
Total body	1.60E-03	5.92E-03
EFF DOSE EQUIV*	5.75E-03	2.13E-02
EFF DOSE*	3.20E-03	1.18E-02

*Units of EDE and ED are mSv/MBq or rem/mCi.

Residence Times:

Heart contents	7.00E-03 hr
Kidneys	7.15E-01 hr
Liver	1.90E+00 hr
Lungs	2.40E-02 hr
Spleen	1.21E-01 hr
Thyroid	2.00E-03 hr

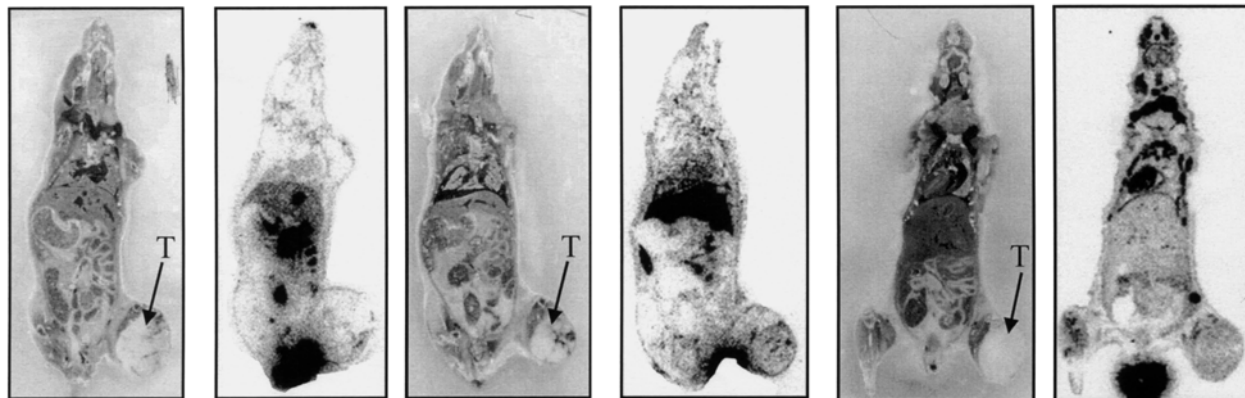


Figure 5. Autoradiography of ^{99m}Tc -EC, ^{99m}Tc -EC-DC, and ^{18}F FDG. Human uterine sarcoma-bearing nude mice were injected with 100 μCi of ^{99m}Tc -EC (left), ^{99m}Tc -EC-DG kit (center), and ^{18}F -FDG (right) and sacrificed 60 minutes postinjection. Sections were cut at 100 μm and exposed for 16 hours. Both ^{99m}Tc -EC-DG and ^{18}F -FDG showed tumor uptake by visualization. Arrow designates tumor site.

apoptotic cells was confirmed by fluorescence microscopy. Immunohistochemical staining (H&E, bFGF, TUNEL, CD31) of tumor tissue after Taxol and cisplatin treatment was also performed, using our previously described procedures.¹⁷

RESULTS

In Vitro [^3H]Thymidine Incorporation and Cell-Cycle Assays

[^3H]Thymidine incorporation assay suggest that EC-DG and glucose incorporated into cell nuclei activity (Fig. 2). FDG showed a decreased uptake in a dose-dependent manner, suggesting either the result of cytotoxic effect or less involvement in cell nuclei activity. Cell sorter assays indicated that ^{99m}Tc -EC-DG was involved in cell-cycle proliferation, whereas ^{18}F -FDG had little or no involvement (Fig. 3).

Effect of Transchelators on Cellular Uptake of ^{99m}Tc -EC-DG Kit

To achieve a high radiochemical yield, transchelators are commonly used in labeling conditions. Gluconate and glucarate, auxiliary chelating agents, were introduced to ^{99m}Tc -EC-DG, and their effect on the cellular uptake of ^{99m}Tc -EC-DG was evaluated. The transchelation preparation of the ^{99m}Tc -EC-DG kit using 10%–40% (w/w) gluconate or glucarate was attempted. The radiochemical yield was >96%. Adding trans-

chelators, such as gluconate and glucarate, did not alter the cellular uptake of ^{99m}Tc -EC-DG (Fig. 4). The findings indicate that gluconate and glucarate play a complimentary role in the stability of ^{99m}Tc -EC-DG during the formulation of the ^{99m}Tc -EC-DG kit.

Dosimetry of ^{99m}Tc -EC-DG Kit in Tumor-bearing Mice

The estimated radiation-absorbed dose is shown in Table 1. If the subject does not involve other radiation exposure, whole body, kidneys, liver, and the effective dose equivalent for the proposed single dose at 20–25 mCi (a common dose used in nuclear medicine practice) falls below the limits for 3 rem annual and 5 rem total-dose equivalent, and other organs of single dose at 5 rem annual and total-dose equivalent at 15 rem. The physical amount of EC-DG and radioactive concentration is 50 mg and 50 mCi/mL. The specific activity is 0.6 mCi/ μmol .

Autoradiographic and Gamma Scintigraphic Imaging Studies

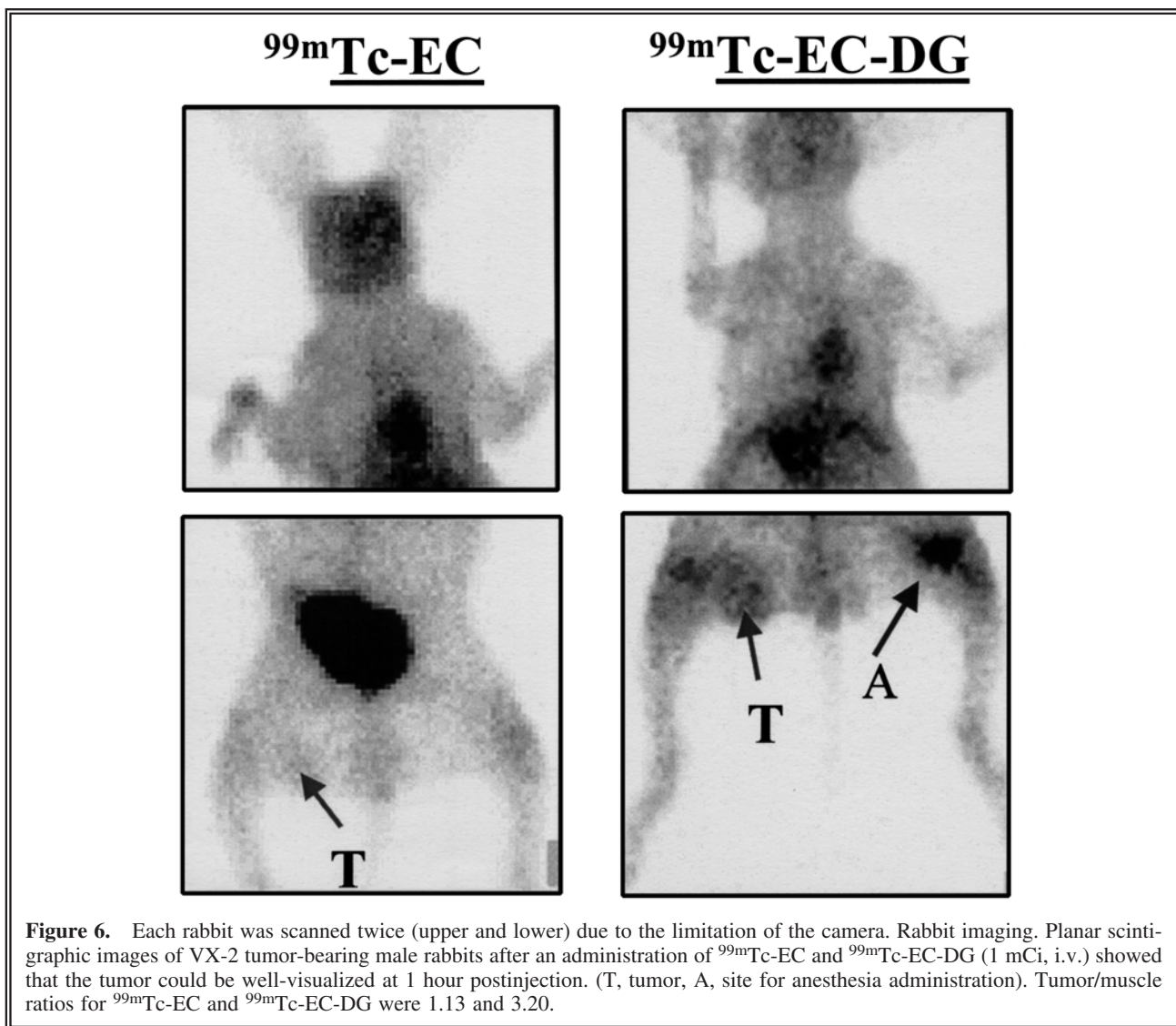
Compared to ^{18}F -FDG autoradiogram, less brain and heart uptake was observed in ^{99m}Tc -EC-DG by visualization. Tumor uptake was well visualized by ^{99m}Tc -EC-DG (Fig. 5). D-glucosamine (DG), an antirheumatic drug exhibiting a natural tropism for cartilaginous tissues, has been labeled with ^{14}C -DG for pharmacokinetic studies.³⁹ Biodistribution and autoradiogram of ^{14}C -DG indicated poor brain and heart uptake, which

showed a similar pattern to our autoradiographic findings. In gamma scintigraphic imaging studies, compared to $^{99m}\text{Tc-EC}$ (control), a tumor could be visualized by $^{99m}\text{Tc-EC-DG}$ in VX-2 tumor-bearing rabbits. For comparative analysis, tumor-to-muscle (counts/pixel, right leg) ratios were determined. Tumor-muscle ratios for $^{99m}\text{Tc-EC}$ and $^{99m}\text{Tc-EC-DG}$ were 1.13 and 3.20 (Fig. 6).

Therapeutic Response Assessment

$^{99m}\text{Tc-EC-DG}$ is capable of measuring tumor-volume changes after Taxol and cisplatin treatment in rodents (Figs. 7–10). An angiogenesis main regulator, such as bFGF expression in solid tumors, was decreased after Taxol treatment, compared to untreated rats (Fig. 8). Cell-cycle analysis indicated specific cell cycle G1 and G2

phase changes and increased apoptosis post-Taxol and cisplatin treatment (Fig. 9). The cells were arrested at the G2 phase after Taxol and cisplatin treatment. A complete remission was observed at 8 mg/kg, whereas a partial remission was noted at 4 mg/kg of CDDP (Fig. 10). ROI analysis showed a marked decrease in tumor-to-muscle ratios (3.16–1.02) post-CDDP treatment in the complete remission group; however, increased tumor-to-muscle ratios (3.27–4.36) were observed in the partial remission group (tumor regrow) on day 39 postinoculation. Immunohistochemistry revealed more viable tumor cells at low-dose than that at high-dose (8 mg/kg) CDDP treatment (Fig. 11). The findings indicated the feasibility of image-guided therapy using $^{99m}\text{Tc-EC-DG}$. Serial imagings are also possible with a



6-hour half-life of ^{99m}Tc to generate increasing retention of ^{99m}Tc -EC-DG in tumors.

DISCUSSION

Assessment of the effectiveness of cancer therapy (e.g., volumetric and morphological changes) is measured by CT and MRI. In addition to these imaging modalities, the treatment endpoints rely almost exclusively on the analysis of biopsies by molecular and histopathological methods. These methods provide a microscopic picture of the general heterogeneous process. Therefore, to assess clinical endpoints adequately, a cell nuclei activity marker is needed that would allow for the precise, spacio-temporal measurement of tumor targets on a whole-body image upon the administration of a functional agent. These mechanism-

based agents provide image-guided therapy, which may discontinue ineffective treatment in the earlier phase and switch to a more efficient treatment that would be beneficial to patients early in the course of treatment.

PET and SPECT use radiotracers to image, map, and measure target-site activities (e.g., angiogenesis, metabolism, apoptosis, and proliferation), and they are considered as molecular imaging modalities. Reliable molecular imaging assays that assess:

- (1) cellular targets at low cost,
- (2) treatment response more rapidly,
- (3) differential diagnosis,
- (4) the prediction of therapeutic response, and
- (5) better dosimetry for internal radiotherapy would be very valuable.

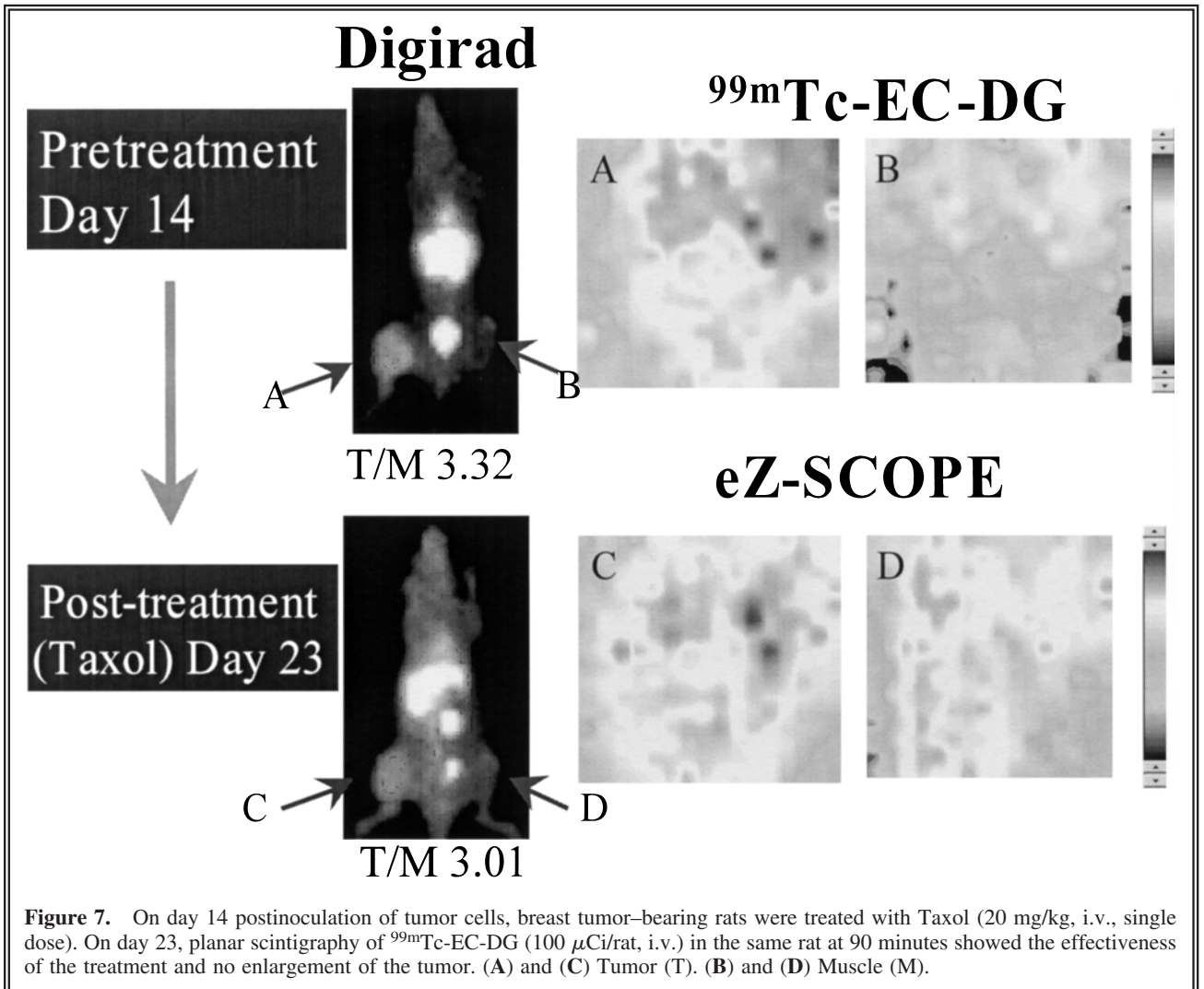


Figure 7. On day 14 postinoculation of tumor cells, breast tumor-bearing rats were treated with Taxol (20 mg/kg, i.v., single dose). On day 23, planar scintigraphy of ^{99m}Tc -EC-DG (100 $\mu\text{Ci}/\text{rat}$, i.v.) in the same rat at 90 minutes showed the effectiveness of the treatment and no enlargement of the tumor. (A) and (C) Tumor (T). (B) and (D) Muscle (M).

Though FDG-PET imaging demonstrates the increased glucose consumption of malignant cells, problems with specificity for cell proliferation have led to the development of new PET tracers. ^{18}F -FDG could assess metabolic activity, but it could not adequately assess cell nuclei activity. Thus, ^{18}F -FDG imaging could not differentiate infection/inflammation from tumor recurrence. Serial imagings have been proposed to measure a greater retention of FDG in tumors, but they are practically limited with a 2-hour half-life of ^{18}F . To develop a tumor-specific agent, it is necessary to assess cell nuclei activity. An assessment of cell nuclei activity provides potential applications in differential diagnosis and the prediction of early treatment response.

Previously, we have reported that the tumor uptake of $^{99\text{m}}\text{Tc}$ -EC-DG is by a glucose-mediated process.¹⁹ Autoradiograms and planar imaging studies showed that there was less brain uptake in $^{99\text{m}}\text{Tc}$ -EC-DG than in ^{18}F -FDG. Poor brain uptake of radiolabeled glucosamine was also reported by others.³⁹ There are at least five glucose

transporters. Glucose transporters 1 and 3 are localized in brain tissue. $^{99\text{m}}\text{Tc}$ -EC-DG may use a different glucose transporter to enter cells.

After completing several experiments, which are illustrated in this paper, there appears to be a strong correlation that EC-DG is involved in cancer cells' synthesis or growth. This conclusion is based on the fact that EC-DG and glucose show similar uptake patterns in the thymidine incorporation assay and that EC-DG is directly involved in the cell-cycle processes (Figs. 2 and 3). EC-DG and glucose are involved in the proliferation/growth activity of the cells. The reason why FDG may not be involved in the growth activity is because of the fluorine atom in position 2 of the molecule, which cannot interact with cytosolic protein. FDG is not directly involved in the cell-cycle processes (Fig. 3). The involvement of EC-DG in the whole cell-cycle pathway would allow for continuous post-treatment follow-ups.

Glucosamine and glucose share the same pathway(s). Whereas glucose may only share 4% of

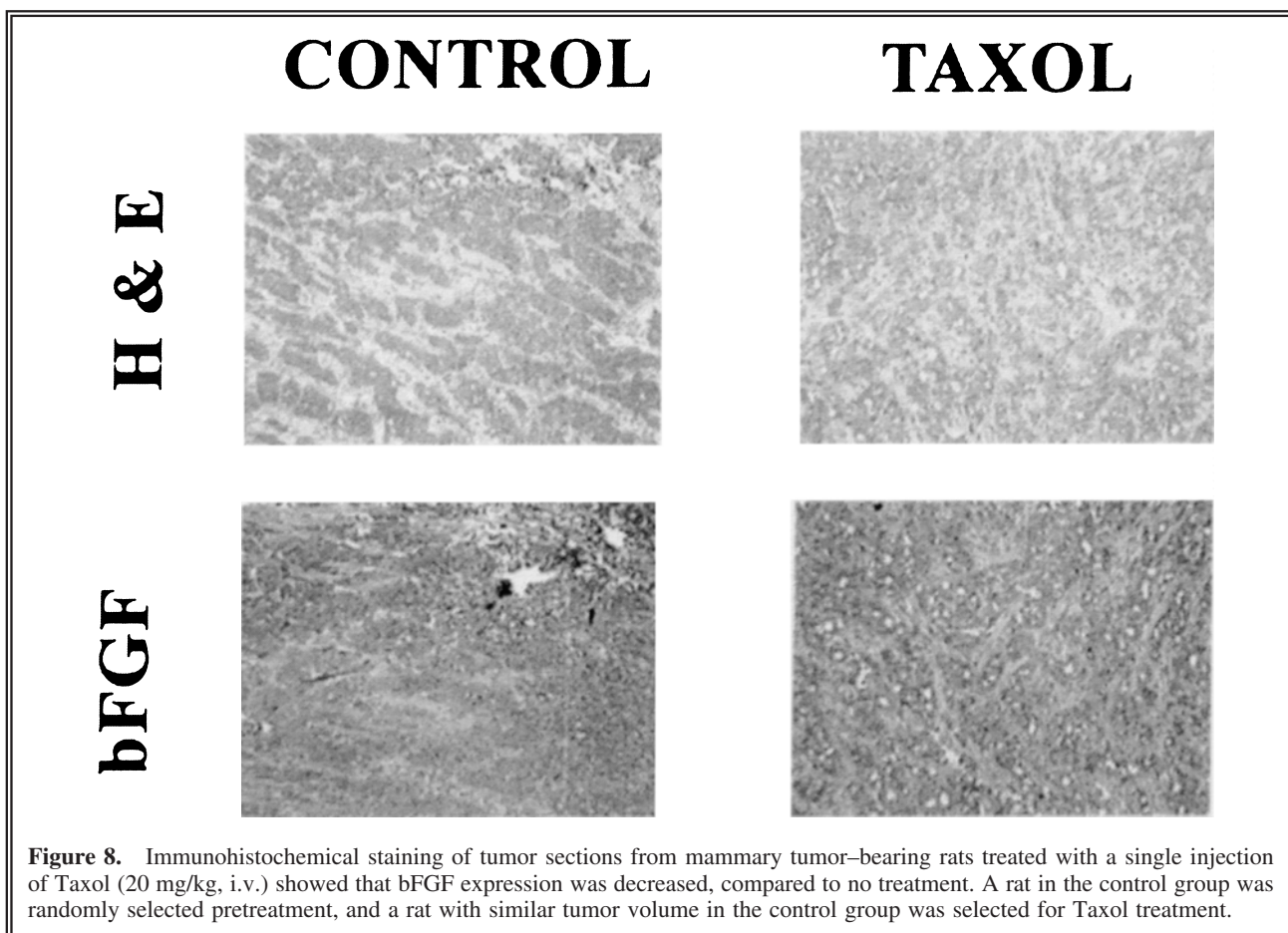


Figure 8. Immunohistochemical staining of tumor sections from mammary tumor-bearing rats treated with a single injection of Taxol (20 mg/kg, i.v.) showed that bFGF expression was decreased, compared to no treatment. A rat in the control group was randomly selected pretreatment, and a rat with similar tumor volume in the control group was selected for Taxol treatment.

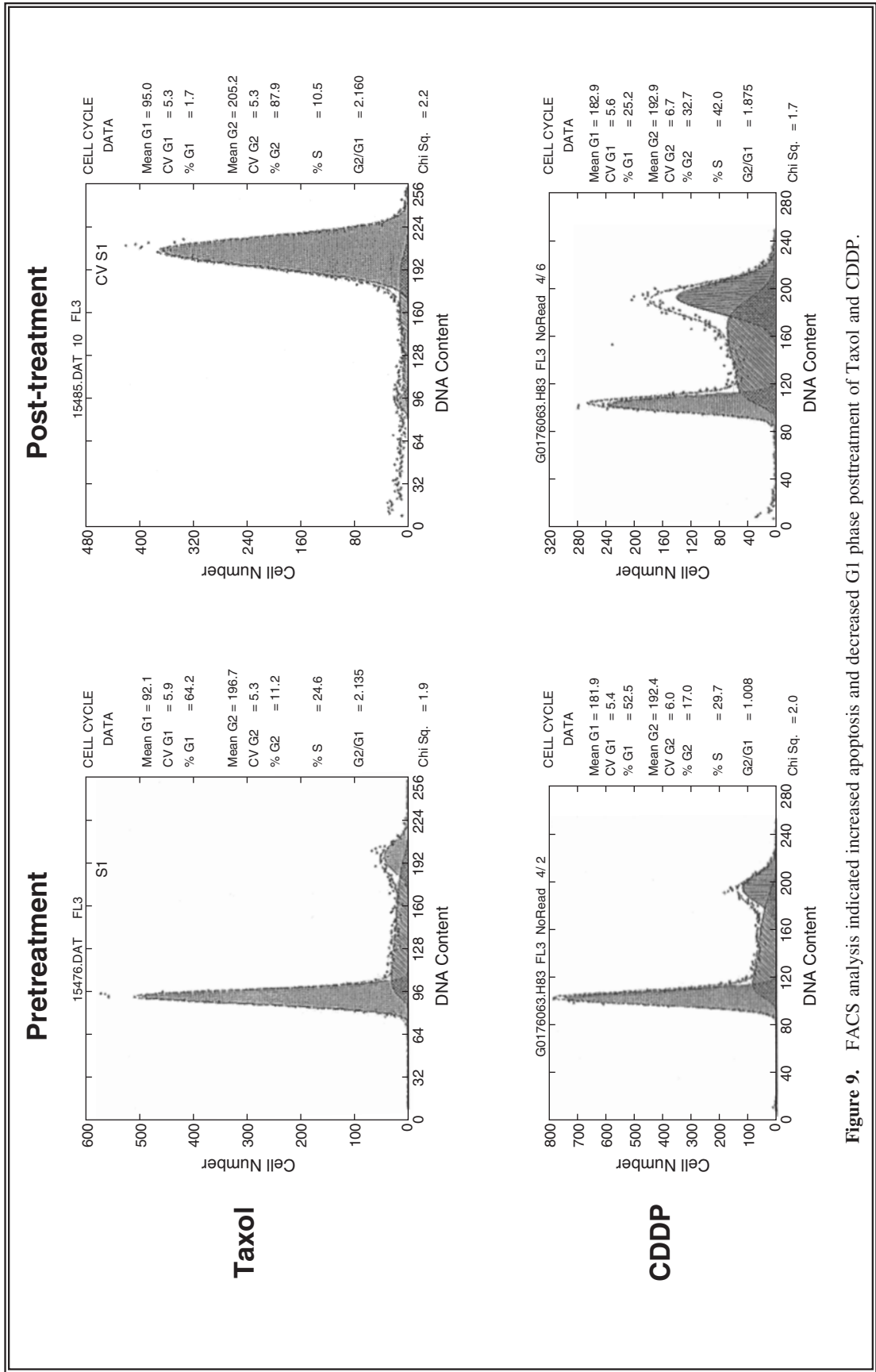
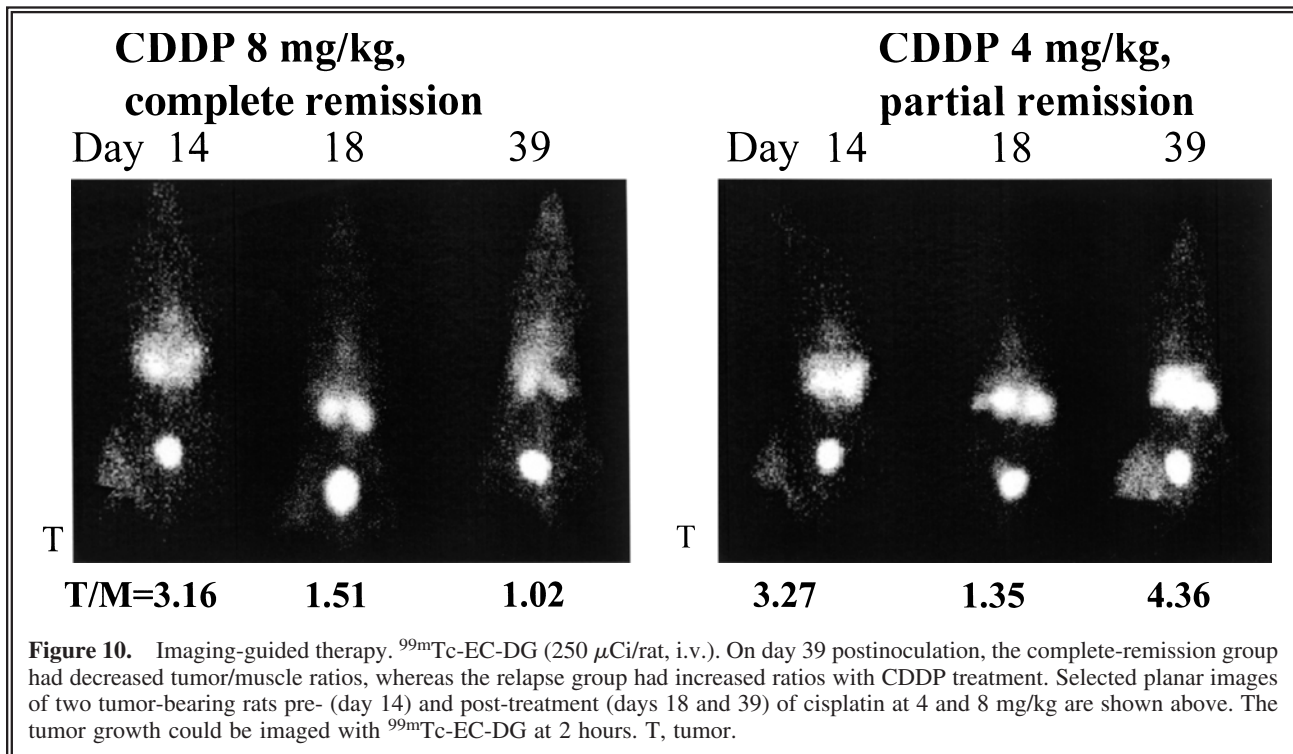
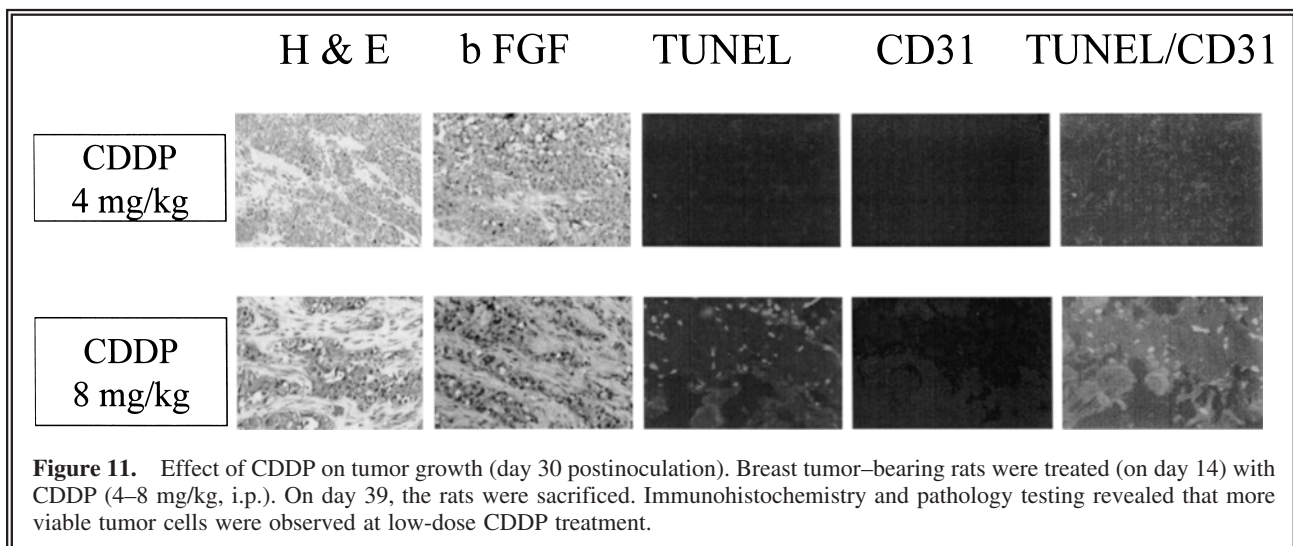


Figure 9. FACS analysis indicated increased apoptosis and decreased G1 phase posttreatment of Taxol and CDDP.



the hexosamine biosynthetic pathway, gluco-
samine is possibly sharing approximately 96% of
both the glycolytic/TCA and the hexosamine
pathways. One reason for this may be that the
molecule (EC-DG) has very key position(s)—for
example, at positions 2 and 6 for D-Glucosamine
and EC, the 2 COO-arms and the 2 dithiols
(SH) locations. During synthesis, the molecule

changes to a peptide linkage, with two sugar arms
with EC linked at position 2 at both sites of the
sugars. EC has formed a peptide-bond linkage
with 2 dithiols, which can react with glycopro-
teins and the lumen of the cell membrane, such
as O-linked N-acetylglucosamine.^{24–27} It is likely
that SH bonds of EC-DG bind to cytosolic
and transmembrane enzymes (Beta-N-acetylglu-



cosaminidase and O-GlcNAc transferase) or membrane-associated proteins (O-linked N-acetylglucosamine), which form (EC-DG)S-S(protein) linkages and support the translocation of EC-DG into the cell nucleus, because it is known that glucosamine is phosphorylated at positions 1 and 6 and binds with uridine diphospho-N-acetylglucosamine to form O-linked N-acetylglucosamine at those same positions, which involves nuclear and cytosolic proteins interaction. Recent studies demonstrate a role for O-GlcNAcylation in processes as diverse as transcription in the nucleus and signaling in the cytoplasm, suggesting that O-GlcNAc has both protein- and site-specific influences on biochemistry and metabolism throughout the cell.^{24,25} We believe that it is this mechanism that is occurring, which makes EC-DG so unique in its ability to be internalized by the cell.

CONCLUSION

In summary, the EC-DG kit can be labeled with ^{99m}Tc easily and efficiently, with high radiochemical purity and is cost-effective. *In vitro* cellular uptake and scintigraphic imaging studies demonstrated the pharmacokinetic distribution and feasibility of using ^{99m}Tc-labeled deoxyglucose for the image-guided therapy of cancer. There was a correlation between tumor uptake and molecular targets (e.g., bFGF, cell cycle) expression. With complex mechanisms expressed in tumor-tissue growth, the technique developed allows for mechanism-specific targeted assessment of cell nuclei activity using ^{99m}Tc-EC-DG.

ACKNOWLEDGMENTS

The authors wish to thank Eloise Daigle for her secretarial support. This work was supported in part by Cell>Point L.L.C., Sponsored Research Grant (MDA LS01-212), and the John S. Dunn Foundation. The animal research was supported by M.D. Anderson Cancer Center (CORE) Grant NIH CA-16672.

REFERENCES

1. Kubota K, Ishiwata K, Kubota R, et al. Tracer feasibility for monitoring tumor radiotherapy: A quadruple tracer study with fluorine-18-fluorodeoxyglucose or

- fluorine-18-fluorodeoxyuridine, L-[Methyl-¹⁴C]methionine, [6-³H]thymidine, and gallium-67. *J Nucl Med* 1991; 32:2118.
2. Tjuvajev J, Muraki A, Ginos J, et al. Iododeoxyuridine uptake and retention as a measure of tumor growth. *J Nucl Med* 1993;34:1152.
3. Strauss LG, Conti PS. The application of PET in clinical oncology. *J Nucl Med* 1991;32:623.
4. Ohtsuki K, Akashi K, Aoka Y, et al. Technetium-99m HYNIC-Annexin V: A potential radiopharmaceutical for the *in vivo* detection of apoptosis. *Eur J Nucl Med* 1999;26:1251.
5. Vriens PW, Blankenberg FG, Stoot JH, et al. The use of technetium ^{99m}Tc Annexin V for *in vivo* imaging of apoptosis during cardiac allograft rejection. *J Thorac Cardiovasc Surg* 1998;116:844.
6. Van Nerom CG, Bormans GM, De Roo MJ, et al. First experience in healthy volunteers with technetium-99m L,L-ethylenedicycysteine, a new renal imaging agent. *Eur J Nucl Med* 1993;20:738.
7. Canet EP, Casali C, Desenfant A, et al. Kinetic characterization of CMD-A2-Gd-DOTA as an intravascular contrast agent for myocardial perfusion measurement with MRI. *Magn Reson Med* 2000;43:403.
8. Laissy JP, Faraggi M, Lebtahi R, et al. Functional evaluation of normal and ischemic kidney by means of gadolinium-DOTA enhanced TurboFLASH MR imaging: A preliminary comparison with ⁹⁹Tc-MAG3 dynamic scintigraphy. *Magn Reson Imaging* 1994;12: w413.
9. Kao CH, ChangLai SP, Chieng PU, et al. Technetium-99m methoxyisobutylisonitrile chest imaging of small-cell lung carcinoma: Relation to patient prognosis and chemotherapy response—a preliminary report. *Cancer* 1998;83:64.
10. Wu HC, Chang CH, Lai MM, et al. Using Tc-99m DMSA renal cortex scan to detect renal damage in women with type 2 diabetes. *J Diabetes Complications* 2003;17:297.
11. Blondeau P, Berse C, Gravel D. Dimerization of an intermediate during the sodium in liquid ammonia reduction of L-thiazolidine-4-carboxylic acid. *Can J Chem* 1967;45:49.
12. Ratner S, Clarke HT. The action of formaldehyde upon cysteine. *J Am Chem Soc* 1937;59:200.
13. Ilgan S, Yang DJ, Higuchi T, et al. ^{99m}Tc-ethylenedicycysteinefolate: A new tumor imaging agent. Synthesis, labeling, and evaluation in animals. *Cancer Biother Radiopharm* 1998;13:427.
14. Zareneyrizi F, Yang DJ, Oh CS, et al. Synthesis of ^{99m}Tc-ethylenedicycysteine-colchicine for evaluation of antiangiogenic effects. *Anti-Cancer Drugs* 1999;10:685.
15. Yang DJ, Ilgan S, Higuchi T, et al. Noninvasive assessment of tumor hypoxia with ^{99m}Tc-labeled metronidazole. *Pharm Res* 1999;16:743.
16. Yang DJ, Azhdarinia A, Wu P, et al. *In vivo* and *in vitro* measurement of apoptosis in breast cancer cells using ^{99m}Tc-EC-Annexin V. *Cancer Biother Radiopharm* 2001;16:73.
17. Yang DJ, Kim K-D, Schechter NR, et al. Assessment

- of antiangiogenic effect using ^{99m}Tc -EC-endostatin. *Cancer Biother Radiopharm* 2002;17:233.
18. Schechter NR, Yang DJ, Azhdarinia A, et al. Assessment of epidermal growth factor receptor with ^{99m}Tc -ethylenedicycysteine-C225 monoclonal antibody. *Anti-Cancer Drugs* 2003;14:49.
 19. Yang DJ, Kim CG, Schechter NR, et al. Imaging with ^{99m}Tc ECDG targeted at the multifunctional glucose transport system: Feasibility study with rodents. *Radiology* 2003;226:465.
 20. Song HC, Bom HS, Cho KH, et al. Prognostication of recovery in patients with acute ischemic stroke through the use of brain SPECT with ^{99m}Tc -labeled metronidazole. *Stroke* 2003;34:982.
 21. Anderson CJ, John CS, Li YJ, et al. N,N'-ethylene-dicycysteine (EC) complexes of Ga(III) and In(III): Molecular modeling, thermodynamic stability, and *in vivo* studies. *Nucl Med Biol* 1995;22:165.
 22. Das T, Banerjee S, Samuel G, et al. [(186/188)Re] rhenium-ethylene dicycysteine (Re-Ec): Preparation and evaluation for possible use in endovascular brachytherapy. *Nucl Med Biol* 2000;27:189.
 23. Li Y, Martell AE, Hancock RD, et al. N,N'-ethylenedicycysteine (EC) and its metal complexes: Synthesis, characterization, crystal structures, and equilibrium constants. *Inorg Chem* 1996;35:404.
 24. Marshall S, Bacote V, Traxinger RR. Discovery of a metabolic pathway mediating glucose-induced desensitization of the glucose transport system. *J Biol Chem* 1991;266:4706.
 25. Wells L, Gao Y, Mahoney JA, et al. Dynamic O-glycosylation of nuclear and cytosolic proteins: Further characterization of the nucleocytoplasmic beta-N-acetylglucosaminidase, O-GlcNAcase. *J Biol Chem* 2002;277:1755.
 26. Pal S, Claffey KP, Cohen HT, et al. Activation of Sp1-mediated vascular permeability factor/vascular endothelial growth factor transcription requires specific interaction with protein kinase C zeta. *J Biol Chem* 1998;273:26277.
 27. Black AR, Black JD, Azizkhan-Clifford J. Sp1 and krupel-like factor family of transcription factors in cell-growth regulation and cancer. *J Cell Physiol* 2001;188:143.
 28. Pedersen MW, Holm S, Lund EL, et al. Coregulation of glucose uptake and vascular endothelial growth factor (VEGF) in two small-cell lung cancer (SCLC) sublines *in vivo* and *in vitro*. *Neoplasia* 2001;3:80.
 29. Hudes GR, Nathan FE, Khater C, et al. Paclitaxel plus estramustine in metastatic hormone-refractory prostate cancer. *Semin Oncol* 1995;22:41.
 30. Pienta KJ. Preclinical mechanisms of action of docetaxel and docetaxel combinations in prostate cancer. *Semin Oncol* 2001;28:3.
 31. Horwitz SB. Mechanism of action of taxol. *Trends Pharmacol Sci* 1992;13:134.
 32. Rowinsky EK, Cazenave LA, Donehower RC. Taxol: A novel investigational antimicrotubule agent. *J Natl Cancer Inst* 1990;82:1247.
 33. Lee LF, Schuerer-Maly CC, Lofquist AK, et al. Taxol-dependent transcriptional activation of IL-8 expression in a subset of human ovarian cancer. *Cancer Res* 1996;56:1303.
 34. Duan Z, Feller AJ, Penson RT, et al. Discovery of differentially expressed genes associated with paclitaxel resistance using cDNA array technology: Analysis of interleukin (IL) 6, IL-8, and monocyte chemoattractant protein 1 in the paclitaxel-resistant phenotype. *Clin Cancer Res* 1999;5:3445.
 35. Lin-Chao S, Chao CC. Reduced inhibition of DNA synthesis and G(2) arrest during the cell cycle of resistant hela cells in response to cis-diamminedichloroplatinum. *J Biomed Sci* 1994r;1:131.
 36. Bose RN. Biomolecular targets for platinum antitumor drugs. *Mini Rev Med Chem* 2002;2:103.
 37. Stabin M. MIRDOSE: The personal computer software for use in internal dose assessment in nuclear medicine. *J Nucl Med* 1996;37:538.
 38. Bunn PA Jr, Helfrich B, Soriano AF, et al. Expression of Her-2/neu in human lung cancer cell lines by immunohistochemistry and fluorescence *in situ* hybridization and its relationship to *in vitro* cytotoxicity by trastuzumab and chemotherapeutic agents. *Clin Cancer Res* 2001;7:3239.
 39. Giraud I, Rapp M, Maurizis JC, et al. Application to a cartilage targeting strategy: Synthesis and *in vivo* biodistribution of (^{14}C)-labeled quaternary ammonium-glucosamine conjugates. *Bioconjug Chem* 2000;11:212.